JMEPEG (2009) 18:49–56
DOI: 10.1007/s11665-008-9253-1

1059-9495/$19.00

Effect of Welding Consumables on Fatigue Performance of Shielded Metal Arc Welded High Strength, Q&T Steel Joints

G. Magudeeswaran, V. Balasubramanian, and G. Madhusudhan Reddy

(Submitted September 3, 2007; in revised form March 17, 2008)

Quenched and Tempered (Q&T) steels are widely used in the construction of military vehicles due to their high strength-to-weight ratio and high hardness. These steels are prone to hydrogen-induced cracking in the heat affected zone (HAZ) after welding. The use of austenitic stainless steel consumables to weld the above steel was the only remedy because of higher solubility for hydrogen in austenitic phase. Recent studies proved that high nickel steel and low hydrogen ferritic steel consumables can be used to weld Q&T steels, which can give very low hydrogen levels in the weld deposits. In this investigation an attempt has been made to study the effect of welding consumables on high cycle fatigue properties of high strength, Q&T steel joints. Three different consumables namely (i) austenitic stainless steel, (ii) low hydrogen ferritic steel, and (iii) high nickel steel have been used to fabricate the joints by shielded metal arc (SMAW) welding process. The joints fabricated using low hydrogen ferritic steel electrodes showed superior fatigue properties than other joints.

Keywords austenitic stainless steel, fatigue properties, high nickel steel, low hydrogen ferritic steel, quenched and tempered steel, shielded metal arc welding process

1. Introduction

Welding has been widely employed in industry as one of the most used methods for connecting components. But due to the heterogeneity induced from welding, base metal (BM), weld metal (WM), and heat affected zone (HAZ) have different mechanical behaviors, which makes welded joints complicated under local stress-strain conditions (Ref 1, 2). For structural steels, the strength of the welded joints determines the strength of the whole structure. Welded joints are subjected to various forms of cyclic loading in practical applications and fatigue failure is common. Thus, welding is a major factor in the fatigue lifetime reduction of components. The assessment of welded joints is a major industrial problem, for two reasons. Firstly, welds tend to be regions of weakness in a structure due to stress concentration effects and poor material properties. Secondly, it is difficult to predict their behavior accurately. This is partly due to the difficulty of defining material properties, which vary throughout the weld and heat-affected zone (HAZ) (Ref 3). Many of the structural components in machines, pressure vessels, transport vehicles, earthmoving equipment, spacecraft, etc. are made of welded joints. The butt welds are the most common in the fabrication and construction of many structures. The wide application of butt welds in various structures, including offshore and nuclear, gives large scope for the researchers to analyze the behavior under different types of loading conditions (Ref 4). Failure analysis of the weldments indicated that fatigue alone is to be considered to account for most of the disruptive failures. Even though the fatigue properties of the weld metal is good, problems can be caused when there is an abrupt change in section caused by excess weld reinforcement, undercut, slag inclusion, and lack of penetration, and nearly 70% of fatigue cracking occurs in the welded joints (Ref 5). Apart from the mechanical considerations of joint design, the welding process, filler material, heat input, number of weld passes, etc. will influence the microstructure of the weld at the joint and in turn will influence the extent of heat affected zone and residual stresses that will build up in the base metal (Ref 6). These factors will invariably affect the fatigue strength by increasing the propensity for crack nucleation and its early growth causing the ultimate failure of the joint. As the fatigue failure is one of the prime concerns in structural design and the butt weld is a part of many structures, its evaluation and prediction of fatigue life is very important to avoid catastrophic failure particularly in steels that are used in military applications.

One of the important criteria for components used in combat vehicle construction is that it should satisfy the ballistic requirements per the requirement. The armor components going into service cannot always be subjected to ballistic proving as it is a destructive type of testing and cannot be performed frequently for all the components. A correlation, therefore, has to be established within limits between ballistic and mechanical properties. Ballistic testing, technically speaking, is just a

G. Magudeeswaran and **V. Balasubramanian**, Centre for Materials Joining & Research (CEMAJOR), Department of Manufacturing Engineering, Annamalai University, Annamalai Nagar 608 002, Tamil Nadu, India; and **G. Madhusudhan Reddy**, Metal Joining Section, Defence Metallurgical Research Laboratory (DMRL), Kanchanbagh (P.O.), Hyderabad 560 058, Andhra Pradesh, India. Contact e-mails: visvabalu@yahoo.com, magudeeswaran@yahoo.com and gmreddy_dmrl@yahoo.com

typical high velocity test of impact behavior of the material, which determines the initial high capacity of energy absorption before cracking and resistance to penetration of a projectile. These two properties mainly depend upon the toughness, i.e., combination of strength and ductility, and hardness of the material. Once the values of impact strength, tensile strength, and hardness of the proved proof welds are known, it can be expected that the armor steel joints will satisfy, within limits, the ballistic standards (Ref 7). The combat vehicles used in military operations will be required to operate under a wide range of road conditions ranging from first class to cross country. Stress loadings within the vehicle hull could be expected to fluctuate considerably and structural cracking especially in welds may become a problem during the service life of these vehicles. To more accurately predict service life, researchers have resorted to fatigue life evaluations in order to simulate actual in-service loading conditions (Ref 8). Thus, an adequate knowledge in tensile and fatigue properties of the armor grade Q&T steel welds is very much essential to meet out the service requirements during the construction of the combat vehicles used in military applications.

Quenched and Tempered (Q&T) steels are widely used in the construction of military vehicles due to its high strength-to-weight ratio and high hardness (Ref 9). These steels are prone to hydrogen induced cracking in the heat affected zone (HAZ) after welding (Ref 10). The use of austenitic stainless steel (ASS) consumables to weld the above steel was the only remedy because of higher solubility for hydrogen in austenitic phase (Ref 11). Recent studies proved that high nickel steel (HNS) and low hydrogen ferritic steel (LHF) consumables can be used to weld Q&T steels, which can give very low hydrogen levels in the weld deposits (Ref 12-14). The use of ASS, HNS, and LHF consumables for armor grade Q&T steel will lead to formation of distinct microstructures in their respective welds. This microstructural heterogeneity will have a drastic influence in the tensile and fatigue properties of the respective welds.

There are no studies in the literature on fatigue testing of similar class of armor grade Q&T steel welds. The present study assumes significance as fatigue studies have not been reported in this class of armor grade Q&T steel welds fabricated using ASS, HNS, and LHF consumables. Thus a study on the effect of welding consumables on fatigue properties will pave way for selection of best welding consumable that meets all the requirements for the construction of combat vehicles. Hence, in this investigation an attempt has been made to compare the high cycle fatigue properties of armor grade Q&T steel joints fabricated by shielded metal arc welding (SMAW) process using austenitic stainless steel, low hydrogen ferritic steel, and high nickel steel electrodes.

2. Experimental Work

The base metal used in this investigation is a Q&T steel, closely confirming to AISI 4340 specification. The microstructural feature of the base metal exhibits acicular martensite (Fig. 1). Rolled plates of 14 mm thick base metal were sliced into the required dimensions (300 mm × 100 mm) by abrasive cutters and grinding. Single 'V' butt joint configuration, as shown in Fig. 2a, was prepared to fabricate the joints by SMAW process. The initial joint configuration was obtained by securing the plates in position using tack welding. The direction

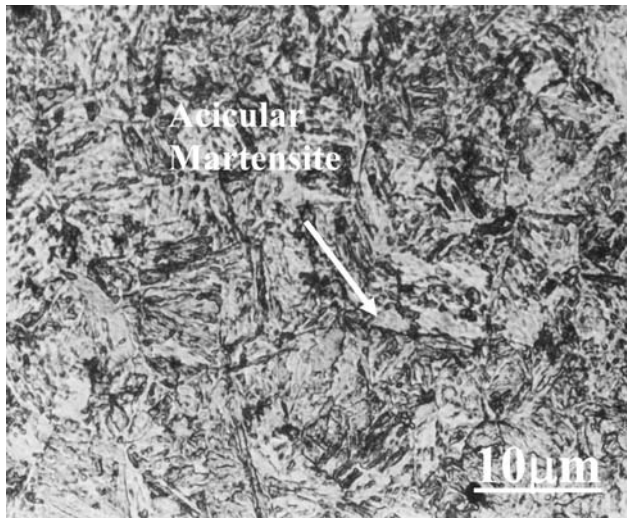

Fig. 1 Microstructure of the base metal

of welding was normal to the rolling direction. All necessary care was taken to avoid joint distortion and the joints were made after clamping the plates in a welding fixture. Austenitic stainless steel (ASS), low hydrogen ferritic steel (LHF), and high nickel steel (HNS) consumables were used to fabricate the joints. The joint fabricated using ASS consumable is referred as SA joint. Similarly, the joint fabricated using LHF consumable is referred as SF joint and the joint fabricated using HNS consumable is referred as SN joint. The chemical composition of the base metal and weld metals were determined using vacuum spectrometer (Model:Spectrolab) and are presented in Table 1.

The process parameters used to fabricate the joints are given in Table 2. The welding procedures (process parameters) followed in this investigation was carried out per guidelines given in the reports (Ref 7, 15) for welding of armor grade Q&T steel used for combat vehicle construction. A detailed weldability test on the armor grade Q&T steel using the filler metals and procedures mentioned in this investigation has been carried out by the authors and has been reported (Ref 16). From this study, it is understood, that the level of diffusible hydrogen content in all the electrodes (ASS, LHF, and HNS) is very much lower than the actual permissible level. The welds made using the above electrodes were offering superior resistance against hydrogen-induced cold cracking if they are fabricated with proper preheat temperature, interpass temperature, electrode baking temperature, etc., as mentioned in Table 2. No evidence of delayed cracking after welding was found in all the welds fabricated using the above welding electrodes and welding procedures and the same has been adopted for welding in this investigation also.

The welded joints were sliced and then machined to the required dimensions (as shown in Fig. 2b-d) for preparing fatigue and tensile test specimens. Two different fatigue specimens were prepared to evaluate the fatigue properties per DIN 50113 specifications. Hourglass type (smooth) specimens were prepared as shown in Fig. 2b to evaluate fatigue limit and notched specimens have been prepared as shown in Fig. 2c to evaluate the fatigue notch factor and notch sensitivity factor. The weld beads of the joints were machined and the effect of bead profile was eliminated in this study. The rotary

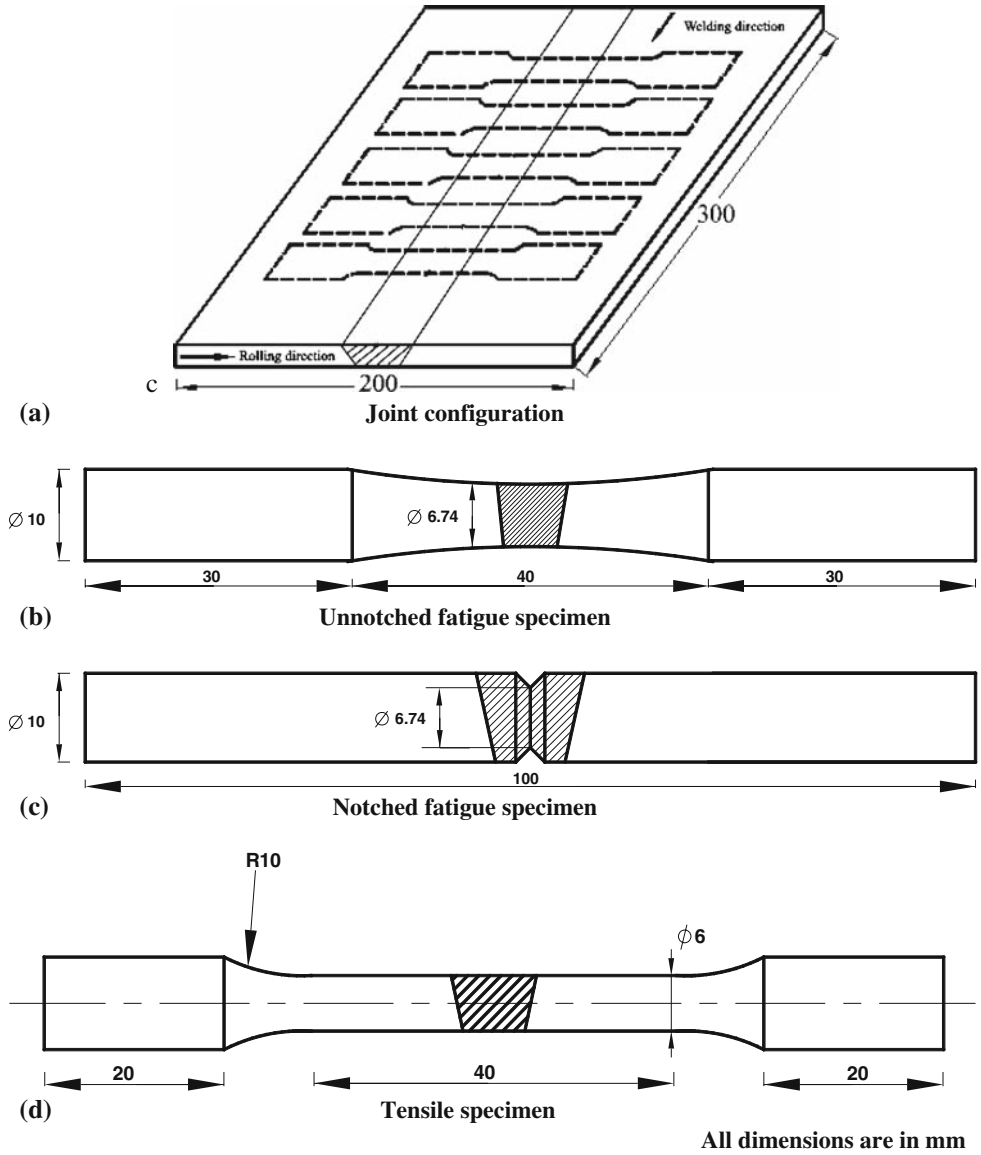

Fig. 2 Joint configuration and test specimen

Table 1 Chemical composition of (wt.%) of base metal and filler metals

Type of material	Notation	C	Si	Mn	P	S	Cr	Mo	Ni	Fe
Base metal										
Armor grade Quenched and tempered steel (Closely confirming to AISI 4340 grade)	BM	0.315	0.239	0.53	0.018	0.009	1.29	0.451	1.54	Bal
Filler metals										
Austenitic stainless steel (Closely confirming to AWS E307)	SA	0.099	0.56	6.59	0.022	0.008	19.614	2.68	9.18	Bal
High nickel electrode steel (AWS ENiCrFe3)	SN	0.0312	0.753	6.45	0.0144	0.001	15.95	0.0173	63	Bal
Low hydrogen ferritic steel (AWS E11018-M)	SF	0.050	0.242	1.30	0.020	0.014	0.133	0.222	2.12	Bal

bending fatigue testing machine (Make: Enkey, India) was used to conduct the experiments at different stress levels and all the experiments were conducted under completely reversed bending load conditions, where mean stress is zero and stress ratio is −1. Tensile specimens have been prepared per ASTM E8M-04 specifications as shown in Fig. 3c to evaluate yield strength, tensile strength, and joint efficiency in accordance with the ANSI/AWS B4.0-98 guidelines for mechanical testing of welds. Tensile test has been carried out in 100 kN, electro-mechanical controlled Universal Testing Machine (Make: FIE-Blue Star, India; Model: 94100). Vicker's microhardness testing machine (Make: Shimadzu; Model: HMV-T1) was used for measuring the hardness across the weld. The microstructure analysis of the weldments was carried out using a light optical

Table 2 Welding conditions

Parameters	Unit	SA	SF	SN
Preheat temperature	°C	100	100	100
Interpass temperature	°C	150	150	150
Electrode baking temperature	°C for 3 h	300	300	300
Filler diameter	mm	4	4	4
Welding current	A	170	160	190
Arc voltage	V	26	23	28
Heat input	kJ/mm	1.60	1.33	1.93

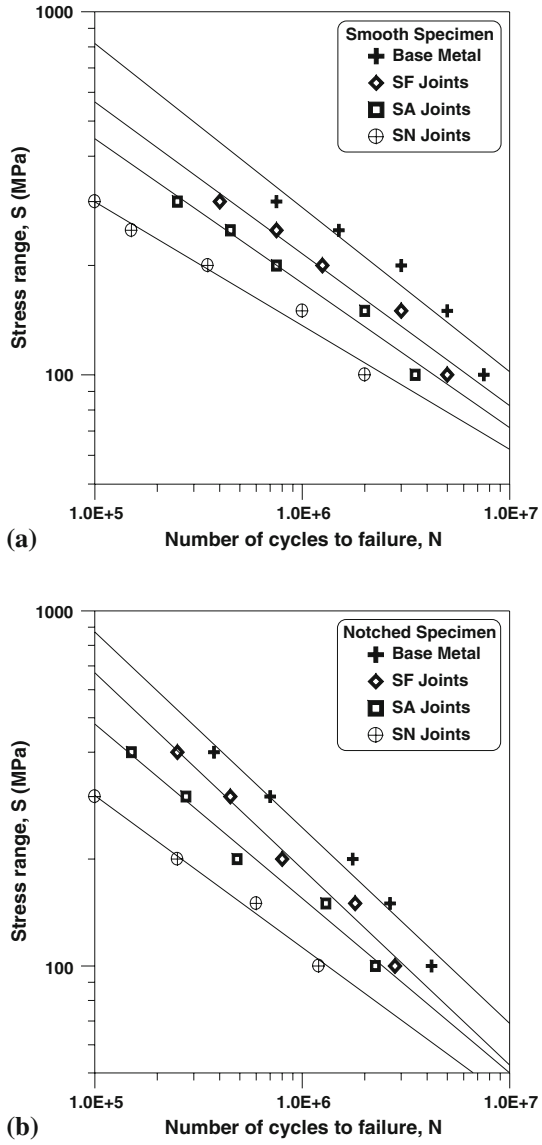

Fig. 3 *S-N* Curves (a) Unnotched specimen (b) Notched specimen

microscope (Make: MEIJI, Japan; Model: ML7100). The specimens were etched with 2% Nital reagent to reveal the microstructure of the weld region of low hydrogen ferritic joint and base metal (BM). Aqua regia and kalling's reagent were used to reveal the microstructure of the austenitic stainless steel weld and high nickel weld regions, respectively.

3. Result

3.1 Fatigue Properties

Three specimens were tested at each stress level and the average of three test results is used to plot *S-N* curves as shown in Fig. 3. The *S-N* curve in the high cycle fatigue region is generally described by the Basquin equation (Ref 17).

$$S^n N = A \quad \text{(Eq 1)}$$

where '*S*' is the stress amplitude, '*N*' is the number of cycles to failure, and '*n*' and '*A*' are empirical constants. Each *S-N* curve shown in Fig. 3 can be represented by the above equation. From those equations, the empirical constants '*n*' (slope of the curve) and '*A*' (intercept of the curve) were evaluated and they are presented in Table 3. When comparing the fatigue strengths of different welded joints subjected to similar loading, it is convenient to express fatigue strength in terms of the stresses corresponding to particular lives, for example 10^5, 10^6, and 10^7 cycles on the mean *S-N* curve. The choice of reference life is quite arbitrary. Traditionally, 2×10^6 cycles has been used, and indeed some design codes refer to their *S-N* curves in terms of the corresponding stress range. For these reasons, in this investigation, fatigue strength of welded joints at 2×10^6 cycles are taken as a basis for comparison. The stress corresponding to 2×10^6 cycles is taken as an indication of the endurance limit and it has been evaluated for all the joints and is presented in Table 3 along with the standard deviation of the measured fatigue limit in brackets. The effect of notches on fatigue strength is determined by comparing the *S-N* curves of notched and unnotched specimens. The data for notched specimens are usually plotted in terms of nominal stress based on the net section of the specimen. The effectiveness of the notch in decreasing the fatigue limit is expressed by the fatigue strength reduction factor or fatigue notch factor, K_f. The fatigue notch factor for all the joints was evaluated using the following expression (Ref 17)

$$K_f = (\sigma_{eS})/(\sigma_{eN}) \quad \text{(Eq 2)}$$

where σ_{eS} is the fatigue limit of unnotched specimen and σ_{eN} is the fatigue limit of notched specimen (σ_{eN}). The notch sensitivity of a material in fatigue is expressed by '*q*' and it can be evaluated using the following expression (Ref 17)

$$q = (K_f - 1)/(K_t - 1) \quad \text{(Eq 3)}$$

where K_t is the theoretical stress concentration factor and is the ratio of maximum stress to nominal stress. Using the above expression, fatigue notch sensitivity factor '*q*' was evaluated for all the joints and they are presented in Table 3. A one population *t*-test was carried out to check whether the mean of the fatigue properties reported are same or different. The reported mean fatigue properties are same at 99.95% confidence level.

From the results presented in Table 3, it is inferred that the base metal endured more number of cycles than all the joints. Among the joints, the SF joints exhibited superior fatigue performance and it endured 14% more number of cycles than SA joints. However, SA endured 23% more number of cycles than SN joints in the unnotched conditions. Slope of the *S-N* curve (Basquin Constant) is another measure to understand the fatigue performance of welded joints. If the slope of the *S-N* curve is smaller, then the fatigue life will be higher and vice

Table 3 Fatigue properties of base metal and welded joints (a)

Joint type	Slope of the *S-N* curve (*n*)	Intercept of the *S-N* curve, A	Fatigue limit (σ_{eS}) of smooth specimen at 2×10^6 cycles, MPa	Fatigue limit (σ_{eN}) of notched specimen at 2×10^6 cycles, MPa	Fatigue notch factor (K_f)	Fatigue notch sensitivity factor (q)	Location of failure
BM	2.21	2.77×10^{11}	210 (6.50)	160 (6.11)	1.31	0.124	Center of the specimen
SF	2.39	3.77×10^{11}	180 (7.02)	140 (8.50)	1.28	0.112	Weld region
SA	2.51	4.56×10^{11}	155 (8.54)	115 (9.01)	1.24	0.136	Weld region
SN	2.93	1.8×10^{12}	120 (9.01)	85 (9.53)	1.41	0.164	Weld region

(a) The numbers in the brackets are the standard deviation of the experimental results

Table 4 Transverse tensile properties of base metal and welded joints (a)

Joint type	Yield strength, MPa	Tensile strength, MPa	Joint efficiency, %	Location of failure
BM	1200 (3.60)	1290 (3.05)	···	Center of the specimen
SA	620 (3.05)	650 (3.21)	50	Weld region
SN	540 (3.60)	620 (3.48)	48	Weld region
SF	830 (3.05)	860 (3.51)	66	Weld region

(a) The numbers in the brackets are the standard deviation of the experimental results

Table 5 Microhardness (VHN) values (0.5 kg load) (a)

Joint type	Location	
	Weld metal region	Base metal region
SA	261 (2.28)	456 (2.52)
SF	311 (2.05)	457 (2.78)
SN	202 (1.87)	453 (2.63)

(a) The numbers in the brackets are the standard deviation of the measured microhardness values

versa. Thus, SF joint with a minimum slope (2.39) exhibits maximum endurance stress of 180 MPa than other joints. Thus, the joints fabricated using low hydrogen ferritic steel consumables exhibited superior performance than the joints fabricated using austenitic stainless steel and high nickel steel in unnotched conditions. Reduction in fatigue strength due to the presence of circular V-notch was evaluated by fatigue notch factor and the notch sensitivity factor. The fatigue notch factor for BM, SF, SA, and SN joints are 1.31, 1.28, 1.24, and 1.41, respectively. Similarly the notch sensitivity factor for BM, SF, SA, and SN joints are 0.124, 0.112, 0.136, and 0.164, respectively. Although the base metal exhibited maximum endurance stress than all other joints, the notch sensitivity factor of the SN joints was found to be the maximum than all other joints. The notch sensitivity factors for joints fabricated using austenitic stainless steel consumables are found to be marginally higher than the joints fabricated using low hydrogen ferritic steel consumables.

3.2 Transverse Tensile Properties

The transverse tensile properties such as yield strength, tensile strength, and joint efficiency of joints were evaluated. In each joint, three specimens were prepared and tested, and the average of the three results is presented in Table 4 along with their respective standard deviation represented in brackets. The yield strength and tensile strength of the base metal are 1200 MPa and 1290 MPa, respectively. The yield strength and tensile strength of SA joint fabricated using austenitic stainless steel electrode are 620 MPa and 650 MPa, respectively, and it indicates that there is 50% reduction in strength due to welding using austenitic stainless steel electrodes. The yield strength and tensile strength of SN joint fabricated using high nickel steel electrode are 540 MPa and 620 MPa and it is clear that there is a reduction in strength by 55% compared to base metal. The SF joint fabricated using low hydrogen type ferritic steel electrode shows an yield strength of 830 MPa and tensile strength of 860 MPa. This also indicates that there is a 39% reduction in strength compared to base metal. Of the three joints, SF joint exhibits 24% higher tensile strength than SA joint and 27% higher than SN joint. Joint efficiency is the ratio between tensile strength of welded joint and tensile strength of unwelded parent metal. The SF joint exhibits a joint efficiency of 66%, whereas the joint efficiency of SA joint is 50% and SN joint is 48%.

3.3 Hardness and Microstructure

Almost all the fatigue and tensile specimens failed in the weld region. Hence, the microhardness measurements and microstructural examinations were done only in the weld metal region. Vicker's microhardness testing machine was used to measure the weld metal hardness, and the values are presented in Table 5. The standard deviations for the measured microhardness values in each case are presented in brackets in Table 5. The hardness of the unwelded base metal is 455 VHN. However, the SA joint exhibits hardness of 261 VHN, SF joint shows 311 VHN, and a hardness of 202 VHN is recorded in SN joint in the weld metal region. The SF joint has 50 VHN more than SA joint and 109 VHN than SN joint in the weld metal region. However, the SA joint has 59 VHN more than the SN joint in the weld metal region. The micrographs of the weld metal regions are displayed in Fig. 4. The micrograph, taken at the weld metal region of the SA joint, exhibits a fine skeletal delta ferrite in plain austenitic matrix (Fig. 4a); the SF joint shows acicular ferrite morphology (Fig. 4b); the SN joint reveals plain austenitic matrix with a scattered delta ferrite matrix (Fig. 4c).

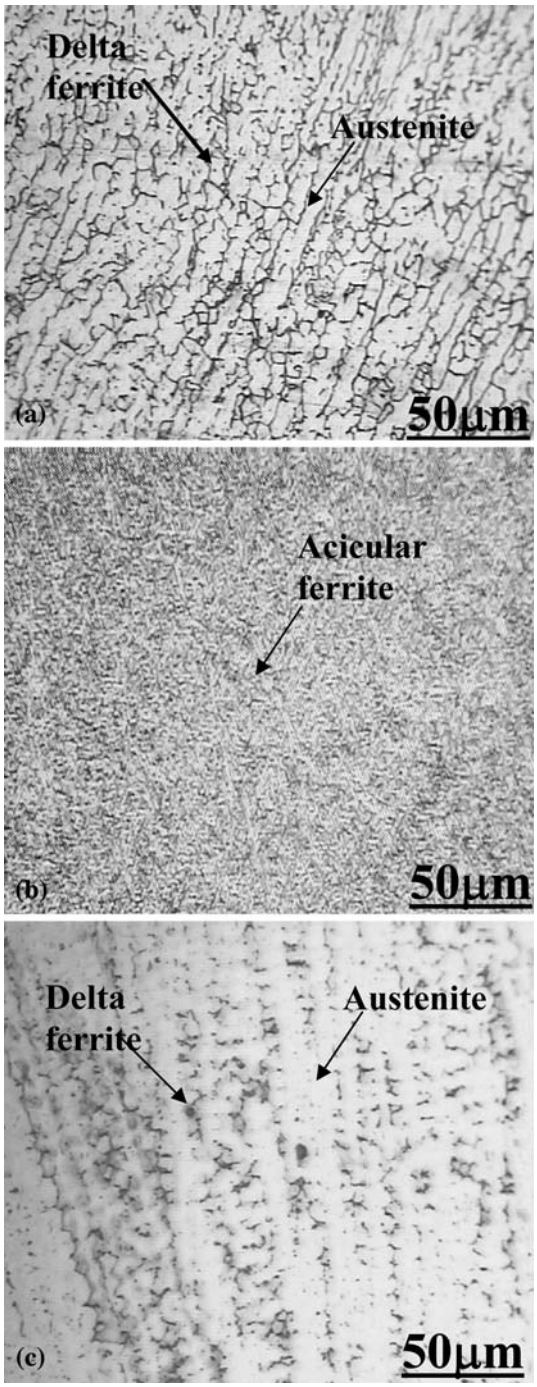

Fig. 4 Optical micrographs of weld metal region (a) SA Joint; (b) SF Joint; (c) SN Joint

4. Discussion

The use of low hydrogen ferritic steel consumables for welding armor grade Q&T steels improved the fatigue performances of the joints compared to the joints fabricated by using conventional austenitic stainless steel consumables and high nickel steel consumables. The basic reason for the improvement in fatigue properties is due to the presence of preferential acicular ferrite type of microstructure which aids for superior transverse tensile properties and weld metal hardness, thereby increasing fatigue resistance of the joints.

4.1 Effect of Welding Consumables on Fatigue Properties of the Joints

The best combination of strength and ductility seems to be possible in the presence of ferrite microstructure. These ferrite structures are very much desirable in all the welded structures as they have relatively higher hardness and strength (Ref 18). Fine grained acicular ferrite structure in weld metal microstructure is desirable than any other form of ferrite phase (Ref 19). The term acicular is used frequently in welds where ferrite plates are relatively small and cover a large proportion of the matrix. A good combination of strength and toughness of low-carbon steel welds is achieved by so-called acicular ferrite microstructure, consisting of small interweaving ferrite plates formed within austenite grains (Ref 20). An acicular ferrite microstructure has the potential of combining high strength and high toughness. This is because the plates of acicular ferrite nucleate intragranularly on nonmetallic inclusions within large austenite grains, and then radiate in many different orientations from those inclusions whilst maintaining an orientation relationship with the austenite (Ref 21). Acicular ferrite is formed as a result of direct nucleation from the inclusions resulting in randomly oriented short ferrite needles with fine grain size and hence hardness is higher. Moreover, acicular ferrite is characterized by high angle boundaries between ferrite grains (Ref 22). The acicular ferrite in the weld metal regions caused repeated deflection and branching of the propagating fatigue crack, thereby reducing the effective stress intensity conditions at the crack tip and retarding crack growth rates in these regions (Ref 23).

It is well known that nickel in weld metal plays important role in microstructural control. It has been reported that the weld metal toughness can be increased appreciably by an increase of Ni content (Ref 24). The higher nickel content reduces the ferrite content of the weld (magnetic microstructural phase and more brittle than austenite), and the nickel additions increase the toughness in fully austenitic compositions thereby reducing the transverse tensile strength. A secondary benefit is that nickel stabilizes austenitic structure against the formation of martensite (another magnetic microstructural phase) (Ref 25). However, some investigations have shown that the benefit from nickel is conditional and it depends upon further alloying elements like manganese (Ref 26). The alloying content of manganese and nickel are very important in the solidification process in high strength steel weld metals. Large additions of these elements can prevent the formation of δ-ferrite entirely, and instead the weld metal solidifies directly to austenite. An additional effect of manganese is that it gives strengthening through solid solution hardening and grain refinement by lowering the austenite to ferrite transformation temperature. Grain refinement also leads to increased toughness. Another important alloying element in austenitic stainless steel and the high nickel steel is chromium. Chromium stabilizes ferrite but slows down transformation rate. With chromium additions, toughness falls as reported in studies of mechanical properties of high strength steel weld metals (Ref 27).

The weld metal chemistry of SN weld metal shows the presence of nickel 63 (wt.%) and chromium 15.95 (wt.%), whereas SA weld metal has 9.18 (wt.%) of nickel and

19.614 (wt.%) of chromium. Higher nickel content promotes the formation of rich austenitic phase in weld metal region. The rich austenitic phase in the weld metal region has a significant influence on the performance of the joints. The SN weld metal region has much higher nickel content than SA weld metal region and it has a direct influence in the microstructure. The micrograph, taken at the weld metal region of the SA joint, exhibits a fine skeletal delta ferrite in plain austenitic matrix, whereas the SN joint reveals plain austenitic matrix with a scattered delta ferrite matrix. Thus, the presence of rich austenitic phase in SA and SN weld metal region reduces the transverse tensile strength and weld metal hardness when compared with that of SF joints. On the other hand, the high nickel content also prevents the formation of the delta ferrite. Delta ferrite is the primary solidification product, i.e., it forms directly from the molten metal. The delta ferrite at the core of the dendrites, which form at the beginning of solidification, is very rich in chromium; the chromium content however goes on decreasing as the solidification proceeds. Proper control of the amount of delta ferrite in welds is very much essential and critical for better performance of the joint (Ref 28). Delta ferrite is not a desirable structure in welds compared with other forms of ferrite when mechanical performance of the joint is concerned. Both the SA and SN type of joints have higher proportion of austenitic phase with inbuilt features of delta ferrite. Thus, SA and SN joints have inferior transverse tensile properties and weld metal hardness and hence poor fatigue resistance than SF joints. Hence, welds with acicular ferrite type of morphology will have higher hardness and yield strength. The SF joint exhibits superior fatigue properties due to the presence of acicular ferrite morphology in the weld metal.

4.2 Effect of Weld Metal Strength on Fatigue Behavior of the Joints

The tensile properties (yield strength, tensile strength, and elongation) of SF joints fabricated using LHF consumables are superior when compared to their ASS and HNS counterparts (see Table 5). Higher yield strength and tensile strength of the SF joints are greatly used to enhance the endurance limit of the joints, and hence the fatigue crack initiation is delayed. Larger elongation (higher ductility) of the SF joints also imparts greater resistance to fatigue crack propagation, and hence fatigue failure is delayed. The combined effect of higher yield strength and higher ductility of the SF joints offers enhanced resistance to crack initiation and crack propagation, and hence the fatigue performance of the joints is superior when compared to SA and SN joints. In the lower strength weld metal, as in the case of joints fabricated using SA and HNS consumables, since the deformation and the yielding are mainly concentrated in the weld metal zone, the extension of the plastic zone is limited within the weld metal. As soon as the plastic zone reaches the fusion line, plasticity keeps on developing along the interface between the parent material and the weld metal (Ref 29). The triaxial state of stress is high in the weld metal and the relaxation of this stress is poor. The crack driving force needed for crack extension is small. So, the fracture toughness of the lower strength weld metal is not high. On the other hand, if the strength of the weld metal is higher, the plastic zone can easily extend into the parent material because the deformation and yielding occur in both weld metal and the base metal. The stress relaxation can easily take place in the crack tip region. So more crack driving force is needed for crack extension, and the fracture resistance of the higher strength weld metal is greater than the lower strength weld metal (Ref 30). This is also one of the reasons for better fatigue resistance of the SF joints. In general, fatigue strength is seriously reduced by the introduction of stress raisers as a notch or hole. The presence of a notch in a specimen under uniaxial load introduces three effects: (i) there is an increase or concentration of stress at the root of the notch; (ii) a stress gradient is set up from the root of the notch toward the center of the specimen; and (iii) a triaxial state of stress is produced (Ref 31). A material which experiences no reduction in fatigue strength due to a notch ($K_f = 1$) has a factor of $q = 0$, while a material in which the notch has its full theoretical effect ($K_f = K_t$) has a factor of $q = 1$. But, 'q' is not a true material constant since it varies with the severity and type of notch, the size of the specimen, and the type of loading. However, it has been proved earlier that the notch sensitivity increases with tensile strength and fatigue notch factor is higher for stronger materials (Ref 32). It is also evident from fatigue test results that higher strength SF joints are more sensitive to fatigue notches and lower strength SA and SN joints are less sensitive to fatigue notches.

5. Conclusions

The effects of welding consumables on fatigue properties of armor grade Q&T joints fabricated by SMAW process have been analyzed in detail. From this investigation, the following conclusions are derived:

1. The use of low hydrogen ferritic steel consumables is found to be beneficial to enhance the fatigue resistance of armor grade Q&T steel joints. An increment of 13% higher fatigue life has been recorded in these joints compared to the joints fabricated by conventional austenitic stainless steel consumables.
2. The superior mechanical properties (higher yield strength and hardness) and preferred microstructures in the weld metal region (acicular ferrite) are the reasons for superior fatigue performance of the joints fabricated using low hydrogen ferritic steel consumables than the joints fabricated using austenitic stainless steel consumables.

Acknowledgments

The authors are thankful to Armament Research Board (ARMREB), New Delhi for funding this project work (Project No. MAA/03/41), M/s Combat Vehicle Research Development Establishment (CVRDE), Avadi, Chennai for providing base material and extending fabrication facility for joint fabrication and Department of Manufacturing Engineering, Annamalai University, for providing testing facility for this investigation.

References

1. D. Radaj, C.M. Sonsino, and D. Flade, Prediction of Service Fatigue Strength of a Welded Tubular Joint on the Basis of the Notch Strain Approach, *Int. J. Fatigue*, 1998, **20**, p 471–480
2. T.L. Teng, C.P. Fung, and P.H. Chang, Effect of Residual Stresses on the Fatigue of Butt Joints Using Thermal Elasto-plastic and Multiaxial Fatigue Theory, *Eng. Fail. Anal.*, 2003, **10**, p 131–151

3. D. Taylor, N. Barrett, and G. Lucano, Some New Methods for Predicting Fatigue in Welded Joints, *Int. J. Fatigue*, 2002, **24**, p 509–518
4. V.V. Yakubovski and I.I. Valteris, Geometrical Parameters of Butt and Fillet Welds and Their Influence on the Welded Joint Fatigue Life, *Int. Inst. Weld. Doc.*, 1989, (No. XIII), p 1326–1369
5. C. Miki and M. Sukano, A Survey of Fatigue Cracking Experience Steel Bridges, *Int. Inst. Weld. Doc.*, 1990, (No. XIII), p 1383–1390
6. I. Easterling, Computer Modeling of Weld Implant Testing, *Mater. Sci. Technol.*, 1985, **1**, p 405–411
7. B. Gupta, *Indian Armour Steel—A Review, Technical Report*. Combat Vehicle Research Development, Chennai, India, 1974, p 2–30
8. M.Z. Shah Khan, S.J. Alkemade, G.M. Weston, and D.G. Wiese, Variable-amplitude Fatigue Testing of a High Hardness Armour Steel, *Int. J. Fatigue*, 1998, **20**(3), p 233–239
9. N. Yurioka, Impact of Welding Research on Steel Composition and Development, *Mater. Design*, 1985, **6**(4), p 154–171
10. F Ade, Ballistic Qualification of Armour Steel Weldments, *Weld. J.*, 1991, **70**, p 53–54
11. G. Madhusudhan Reddy, T. Mohandas, and G.R.N. Tagore, Weldability Studies on High-strength Low-alloy Steel Using Austenitic Stainless Steel Filler, *J. Mater. Process. Technol.*, 1995, **49**, p 213–228
12. S.J. Alkemade, *The Weld Cracking Susceptibility of High Hardness Armour Steel*. Defense Science and Technology Organization, Australia (AR No: 009-659), 1996, p 1–17
13. G. Madhusudhan Reddy, T. Mohandas, and D.S. Sarma, Cold Cracking Studies on Low Alloy Steel Weldments; Effect of Filler Metal Composition, *Sci. Technol. Weld. Join.*, 2003, **8**(6), p 407–414
14. M.D. Rowe, T.W. Nelson, and J.C. Lippold, Hydrogen-induced Cracking Along Fusion Boundary of Dissimilar Metal Welds, *Weld. J.*, 1999, **2**, p 31s–37s
15. N. Ramakrishnan, *Ballistic Test Procedures for Armour Materials*. Technical Report Defence Metallurgical Laboratory, Hyderabad, India, 1996, p 24–39
16. G. Magudeeswaran, V. Balsubramanian, and G. Madhusudhan Reddy, Effect of Welding Consumables on Hydrogen Induced Cracking of Armour Grade Quenched and Tempered Steel Welds, *Ironmak. Steelmak. Prod. Appl.*, 2008, in press
17. E. DieterGeorge, *Mechanical Metallurgy*. 3rd ed., McGraw-Hill Publishing, New York, 1988, p 376–431
18. W. Juan and L. Yajiang, Microstructure Characterization in the Weld Metals of HQ130 +QJ63 High Strength Steels, *Bull. Mater. Sci.*, 2003, **36**(3), p 35–39, Indian Academy of Science
19. A.J. Pacey and H.W. Keer, Quantitative Microstructural Studies of Submerged Arc Welds in HSLA Steels, *Proceedings of the 5th Bolton Landing Conference*, 1978, p 285–303
20. F.J. Barbaro, P. Krauklis, and K.E. Easterling, Formation of Acicular Ferrite at Oxide Particles in Steels, *Mater. Sci. Technol.*, 1989, **5**, p 1057–1068
21. F. Xiao, B. Lia, D. Ren, Y. Shan, and K. Yang, Acicular Ferritic Microstructure of a Low-carbon Mn-Mo-Nb Microalloyed Pipeline Steel, *Mater. Charact.*, 2005, **54**, p 305–314
22. R.A. Howell and G.S. Barritte, The Nature of Acicular Ferrite in HSLA Steel Weld Metals, *J. Mater. Sci.*, 1982, **17**, p 732–740
23. P.E. Bratz, B.L. Braglia, and R.W. Hertzberg, Fatigue Behaviour of HSLA Steel and Associated Weldments, *Proceedings of the 5th Bolton Landing Conference*, 1978, p 271–284
24. J.D. Parker and G.C. Stratford, Review of Factors Affecting Condition Assessment of Nickel Based Transition Joints, *Sci. Technol. Weld. Join.*, 1999, **4**(1), p 29–39
25. T.A. Siewert, How to Predict Impact Energy from Stainless Steel Weld Composition, *Weld. Design Fabric.*, 1978, **57**, p 87–88
26. G. Goodwin, Welding Process Selection for Fabrication of a Superconducting Magnet Structure, *Weld. J.*, 1985, **64**(8), p 19–20
27. L. Schafer, Influence of Delta Ferrite and Dendritic Carbides on the Impact and Tensile Properties of a Martensite Chromium Steel, *J. Nucl. Mater.*, 1998, **258**, p 1336–1339
28. Y.C. Lin and P.Y. Chen, Effect of Nitrogen and Retained Ferrite on Residual Stress in Austenitic Stainless Steel Weldments, *Mater. Sci. Eng. A*, 2001, **307**, p 165–171
29. C. Eripret and P. Hornet, Prediction of Overmatching Effects on the Fracture of Stainless Steel Cracked Welds, *Proceeding of Mis-matching of Welds, ESIS 17*. Mechanical Engineering Publications, London, 1994, p 685–708
30. D.C. Lin, T.S. Wang, and T.S. Srivatsan, A Mechanism for the Formation of Equiaxed Grains of Aluminium-Lithium Alloy 2090, *Mater. Sci. Eng.*, 2003, **A335**, p 304–309
31. R.W. Hertzberg, *Deformation and Fracture Mechanics of Engineering Materials*. John Wiley & Sons, London, 1983
32. H.O. Fuchs and R.I. Stephens, *Metal Fatigue in Engineering*. John Wiley & Sons, London, 1980